AGU PUBLICATIONS

Water Resources Research

RESEARCH ARTICLE
10.1002/2013WR013730

Key Points:
- The use of multiple point statistics for object based simulations
- A meander simulation method based on orientations with 1-D training images
- An inverse conditioning methodology that preserves the meander characteristics

Supporting Information:
- Readme
- Digitized Secure River
- Digitized Purus River
- Digitized Preacher Creek River
- plot_channel
- Digitized Mamore River
- Digitized Little Black River
- Digitized Bubuye River
- Digitized Birch Creek River
- Table S1
- Figures S1, S2, S3, S4, S5, S6, S7, S8, S9, S10, S11, S12, S13, S14, S15, S16, S17, S18, S19, S20, S21, S22
- Videos S1, S2

Correspondence to:
G. Mariethoz,
gregoire.mariethoz@minds.ch

Citation:
Mariethoz, G., A. Comunian, I. Irarrazaval, and P. Renard (2014), Analog-based meandering channel simulation, *Water Resour. Res.*, *50*, 836–854, doi:10.1002/2013WR013730.

Received 22 FEB 2013
Accepted 8 JAN 2014
Accepted article online 11 JAN 2014
Published online 3 FEB 2014

Analog-based meandering channel simulation

Gregoire Mariethoz[1], Alessandro Comunian[2], Inigo Irarrazaval[1], and Philippe Renard[3]

[1]School of Civil and Environmental Engineering, University of New South Wales, Sydney, New South Wales, Australia, [2]School of Biological, Earth and Environmental Sciences, University of New South Wales, Sydney, New South Wales, Australia, [3]Centre of Hydrogeology and Geothermics, University of Neuchâtel, Neuchatel, Switzerland

Abstract Characterizing the complex geometries and the heterogeneity of the deposits in meandering river systems is a long-standing issue for the 3-D modeling of alluvial formations. Such deposits are important sources of accessible groundwater in alluvial aquifers throughout the world and also play a major role as hydrocarbons reservoirs. In this paper, we present a method to generate meandering river centerlines that are stochastic, geologically realistic, connected, and conditioned to local observations or global geomorphological characteristics. The method is based on fast 1-D multiple-point statistics in a transformed curvilinear domain: the succession in directions observed in a real-world meandering river (the analog) is considered as statistical model for multiple-point statistics simulation. The integration of local data is accomplished by an inverse procedure ensuring that the channels pass through a given set of locations while conserving the high-order spatial characteristics of an analog. The methodology is applied on seven real-world case studies. This work demonstrates the flexibility and the applicability of multiple-point statistics outside the standard paradigm that considers the simulation of a 2-D or 3-D variable with spatial coordinates.

1. Introduction

The scientific community has been interested in meandering rivers for a long time, including Leonardo Da Vinci [*Gyr*, 2010; *Einstein*, 1926]. The disciplines involved in their study are wide and include, among others, fluid mechanics, mathematics, hydrogeology, ecology, engineering, and geomorphology. In this paper, we focus on the generation of meandering rivers for applications in reservoir modeling. Meandering rivers are "the most common river planform style in populated areas" [*Crosato*, 2008], therefore, besides attracting purely scientific interests, such environments play a key role in water resources management. Their sedimentary deposits contain sand-filled channels that have high porosity and high hydraulic conductivity, therefore being often considered as productive aquifers [*Castilla-Rho et al*., 2014]. Moreover, similar environments are also studied since reservoirs of fluvial origin host a considerable amount of the current reserves of hydrocarbons [*Deutsch and Wang*, 1996; *Keogh et al*., 2007].

A critical aspect of groundwater resources management is to quantify the uncertainty in flow and transport forecasts in an aquifer. To this, the classical Monte-Carlo approach consists in first obtaining several plausible geological models. In a second step, fluid flow simulation is applied to all these models, resulting in as many forecasts. The multiple forecasts are then used to formulate a probability distribution of the predictions that is the basis for aquifer management decisions. Because the geological model is at the origin of the prediction uncertainty, it is important that the multiple geological models appropriately cover the space of uncertainty of the geological structures. This requires that the models present realistic geological heterogeneity.

Alluvial reservoir is commonly conceptualized as meandering channels bodies of higher hydraulic conductivity in a matrix of lower hydraulic conductivity material [*Deutsch and Tran*, 2002; *Pyrcz et al*., 2009]. From a reservoir engineering point of view, the single most critical and uncertain feature in this type of aquifer is the geometry and the connectivity of the sand bodies or channelized structures. An important challenge in hydrogeology is therefore to characterize the complex geometries, the heterogeneity and the connectivity of these reservoirs [*Renard et al*., 2011; *Renard and Allard*, 2013]. Very often the sand-filled channels lie in a background of less permeable rock type, and the information about their geometry is restricted by what can be grasped from the surface, some borehole logs and geophysical surveys. In addition, a large body of

work has been developed on the conceptualization of alluvial aquifers, based on the observation of present-day meandering river systems. According to the classification of *Koltermann and Gorelick* [1996], approaches for the simulation of heterogeneous subsurface structures can be classified in two main categories: process-imitating approaches (physics-based) and structure-imitating approaches (statistics-based). For the particular case of deposits related to meandering rivers, the existing literature contains a number of approaches falling in these two categories.

A large body of work addresses the physics-based description of meandering rivers. One of the seminal works in this direction was to model the evolution of the meander taking into account the near-bank excess velocity and the planform curvature [*Ikeda et al*., 1981]. The model proposed by *Ikeda et al*. [1981] has been used as reference in many subsequent works [i.e., *Camporeale et al*., 2005; *Darby et al*., 2002; *Howard and Knutson*, 1984; *Stølum*, 1996; *Sun et al*., 1996]. It has been extended to include different sources of instability, for example, related to bank erosion processes [*Seminara*, 2006]. Some of the more recent approaches try to overcome other limitations of the model of *Ikeda et al*. [1981], such as the simplified relationship between the eroding and the deposit banks that entails a constant bankfull width [*Parker et al*., 2011]. These models can reproduce many features of real channels, but they require calibration of empirical parameters, which can be difficult [*Darby et al*., 2002]. Other approaches include the physics of sedimentary processes in a genetic or pseudo genetic stochastic model [*Gross and Small*, 1998; *Lancaster and Bras*, 2002]. In addition, process-based and event-based methods have been recently developed to incorporate the physical evolution of the channel in a stochastic framework [*Lopez*, 2003; *Lopez et al*., 2008; *Pyrcz et al*., 2009]. Although such methods generate very realistic models, they often require a high level of parameterization and present limitations in their conditioning capabilities [*Bertoncello et al*., 2013; *Michael et al*., 2010].

Some models have, however, been proposed that incorporate a random component with the physical rules. For example, *Posner and Duan* [2012] extend the model of *Ikeda et al*. [1981] with a stochastic bank erosion coefficient. Other process-imitating approaches approximate the physics involved in the modeling of meanders with a set of rules ("holistic" approaches according to *Seminara and Pittaluga* [2012]). These approaches are often based on the cellular automata paradigm [*Frisch et al*., 1986]. Several studies have investigated the use of cellular automata for the simulation of rivers [*Coulthard and Van De Wiel*, 2006; *Coulthard et al*., 2007; *Murray and Paola*, 1994, 1997]. One of the main difficulties for the application of these models is the selection of the criteria and the interaction rules used to replace the physics of the phenomena [*Seminara and Pittaluga*, 2012].

The second set of approaches to meander simulation corresponds to structure-imitating methods which are purely stochastic and therefore do not include any physics or geological rules. Such approaches focus on mimicking the statistical properties of known channels, and belong to the broad category of geostatistics. These are mostly used in data-poor cases where the physical parameters of the meandering system are not quantitatively known, but there is a geological interpretation available and a qualitative knowledge of the type of deposition environment. The method proposed in this paper belongs to this category.

A first family of structure-imitating methods is Boolean models which define the location of a channel centroid by random parameters describing characteristics such as the channel centerline, the deviation of the channel from this centerline, the channel sinuosity, etc. Examples of this approach can be found, for example, in *Deutsch and Wang* [1996], *Georgsen and Omre* [1993], *Haldorsen and Chang* [1986], and *Langbein and Leopold* [1966]. Object-based models, however, can lack flexibility because they are limited to a given set of fixed geometries, not fully representative of the variability found in subsurface structures. Moreover, they can be difficult to condition to dense data sets. Variogram-based models have also been used to model channelized structures [*Schlüter and Vogel*, 2011; *Zinn and Harvey*, 2003], although their application is difficult due to inherent assumptions of maximum entropy and Gaussianity. Another geostatistical approach is multiple-point statistics (MPS) [*Hu and Chugunova*, 2008; *Strebelle*, 2002], which was originally developed to address the issue of geological realism and connectivity of stochastic structures. MPS uses training images as a model of spatial variability. Training images are explicit representations, or examples that are considered as analogs for the studied phenomenon, and are used as a source of spatial patterns for the structures to represent. A main motivation for the use of training image is to inject expert knowledge in cases where the data alone is too sparse to infer what type of spatial variability is present in the subsurface. However, a paradox of MPS is that currently it typically fails to reproduce some highly connected patterns. Some fixes have been proposed, mostly consisting of postprocessing algorithms [*Stien et al*., 2007; *Strebelle and Remy*,

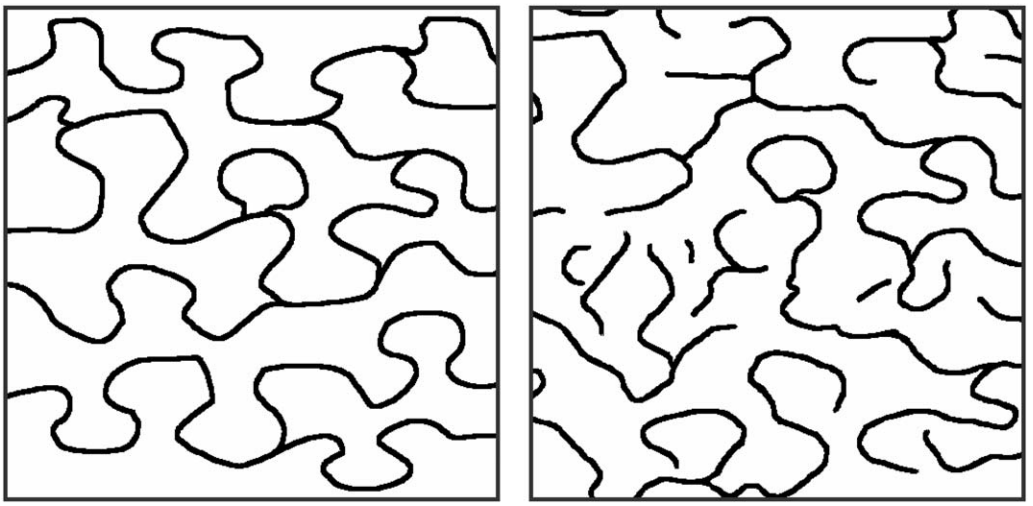

Figure 1. Example of a simulation of highly sinuous meanders using MPS. (left) Training image. (right) One realization with disconnected structures [realization obtained with the direct sampling algorithm, *Mariethoz et al*., 2010b], parameters: $n = 60$, $t = 0$, $f = 1$).

2005; *Suzuki and Strebelle*, 2007]. The problem, however, remains acute when representing thin, sinuous structures, such as typically found in meandering systems or karstic aquifers. Figure 1 shows an example of a simulation produced using MPS, based on a training image that presents such thin connected meandering channels. The connectivity of the structures is in this case not correctly preserved, which can drastically affect, for example, flow and transport processes [*Klise et al*., 2009; *Le Coz et al*., 2011].

In the same domain of structure-imitating approaches, *Surkan and Van Kan* [1969] propose to simulate the channel centerline as a random walk, where the direction of the path is a statistical function of a directional property. *Oliver* [2002] developed a similar approach that allows obtaining conditional simulation. This line of research is very interesting because it allows building complex objects which themselves present stochasticity and are conditioned to data. However, the random functions used in those approaches do not allow reproducing features such as the geometric nonlinearity that characterizes many of the real-world meanders [*Bashore et al*., 1994; *Perucca et al*., 2005; *Seminara et al*., 2001], yielding simulated channels that lack realism and present conditioning artifacts.

In this paper, we propose a new methodology for stochastic meanders simulation that combines promising aspects of the random walk-based approaches [*Oliver*, 2002; *Surkan and Van Kan*, 1969] with training image-based methods (MPS) for imposing structures similar to known present-day meanders. It addresses the major limitations of previous methods, which are:

1. realism of the structures modeled;

2. inference of the properties for a given geomorphological setting through an analog-based approach;

3. conditioning to the occurrence of a channel at specific locations (hard conditioning) or to a general direction of the system (soft conditioning).

Realism is achieved by using direct sampling (DS) simulation to generate the succession of directions [*Mariethoz et al*., 2010b]. DS is a multiple-point simulation method that allows dealing with continuous variables, such as the successive directions taken by the meandering channel. The training image consists of a digitized image of a meandering channel, obtained from field mapping or remote sensing (i.e., aerial photographs, Google Earth). Such a training image approach naturally solves the inference problem since it is possible to obtain analog images for a multitude of different depositional environments.

The problem of conditioning to hard and soft data is solved by devising an inverse procedure that iteratively perturbs stochastic models while preserving their high-order statistical properties, based on the iterative spatial resampling (ISR) scheme [*Mariethoz et al*., 2010a]. It is formulated as the minimization of an objective function which provides increased flexibility to integrate different data types and is

computationally feasible thanks to the very small CPU cost of simulating a meandering channel. The method is applied to the simulation of meandering channels for seven case studies located in a variety of environments. For reasons of space, only two case studies are presented in the body of the paper (Birch Creek and Preacher Creek), and exhaustive results on the rest of the case studies are presented in the supporting information (Figures S1–S22, available online).

2. Methodology

Our approach consists of modeling meandering channels centerlines by simulating, with continuous variable multiple-point statistics, a succession of directions as a one-dimensional random process. The centerline of a present-day meandering channel is digitized from a satellite image and interpolated at regularly spaced steps. Note that in the following for simplicity, we use the term "channel" to denote a meandering channel centerline. The succession of directions in the channel from one step to the subsequent are analyzed and used as a statistical model. This statistical model, or 1-D training image in the terminology of multiple-point statistics (training channel), is used in the DS for the simulation of another sequence of directions. This simulated sequence presents the same statistical properties as the training image, and can be used to draw a channel with the same morphological characteristics but with a different centerline. The simulation being a stochastic process, a number of different channels can be obtained from the same training image for characterizing uncertainty.

2.1. Digitizing the Training Image

The first step of the methodology is to digitize an existing meandering channel that is considered an analog of the structures to be modeled. One can identify locations with similar sediment load, slope, and geomorphological setting. An important requirement when choosing an analog channel is that it must be large enough to contain a statistically significant number of spatial patterns to inform the meandering channels generation model. Moreover, the analog channel should also ideally be stationary, meaning that it comprises a river reach where similar processes are taking place. It should therefore be representative of similar areas immediately upstream or downstream or considered at different periods where similar conditions take place. In addition, although we do not investigate nonstationarity in this paper, we note that methods have been developed to use nonstationary training images [*Chugunova and Hu*, 2008; *de Vries et al*., 2009], and there is no technical limitation to use them with our approach.

All example cases considered in this paper use analogs taken from the Google Earth platform, which is ideal for this task. The analog channel is initially manually digitized (Figure 2, blue dots). However, the simulation procedure (described further) requires the channel to be represented as points at fixed intervals. Therefore, the digitized points are interpolated at equidistant locations along the channel using a spline (Figure 2, red crosses). The length of the discretization step is denoted as s. Here we consider that the manually digitized points are close enough not to incur significant uncertainty, and that they are error-free. An alternative to the manual digitization would be to use databases of discretized rivers or to develop a tool to automate the digitization process.

Once a series of equidistant locations is available, the analog meandering channel (training channel) can be represented using three equivalent representations:

An array of N equidistant points of coordinates (x_i, y_i) with $i=1, \ldots, N$.

An array containing the $N-1$ directions θ_i of each segment, given the starting point (x_1, y_1) and the discretization step s.

An array containing the $N-2$ direction-changes $\Delta\theta_i=(\theta_{i+1}-\theta_i)$, given the starting point, the initial direction θ_0 and the discretization steps.

In the following, we use the second notation: the training channel is represented as a series of directions θ_i.

2.2. Morphometric Attributes

Howard and Hemberger [1991] conducted a detailed study on the characterization of meandering channels, and identified a number of morphometric attributes of interest. Those attributes enclose important information about the channel geometry and have been used to discriminate between synthetic and natural

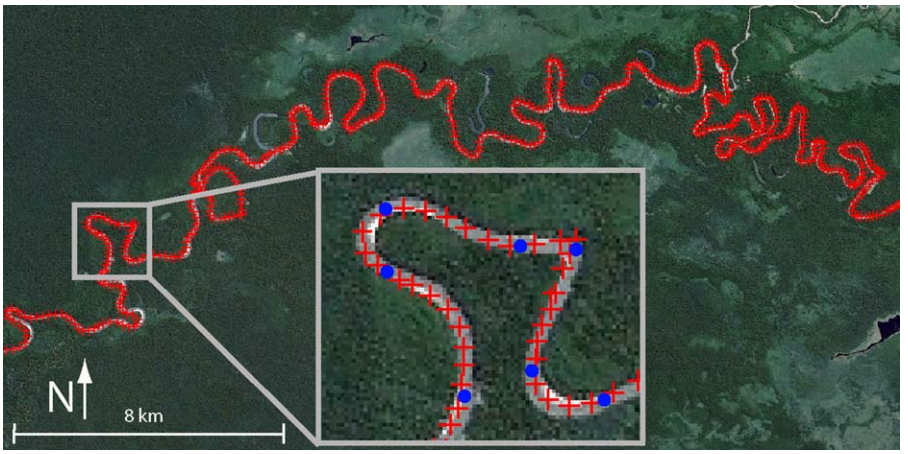

Figure 2. Digitization procedure. Blue dots: original digitized points. Red crosses: spline interpolated points (Source: "Secure river" 15°53′52S and 65°52′23W. Google Earth, 16 October 2013).

channels. Here we evaluate the results of our simulations using some of the attributes considered by *Howard and Hemberger* [1991] together with additional ones, all described hereinafter.

A first group of attributes describe the sinuosity of the channel. The straight-line distance D (Figure 3) can be used to compute the total sinuosity μ_T. If the total length of a channel is defined as $\lambda = sN$, then the total sinuosity is $\mu_T = \lambda/D$. The concept of total sinuosity can be extended by computing it as a moving average on portions of the main channel having different lengths. In this case, the total sinuosity depends on the size of the moving window w and is therefore denoted $\mu_T(w)$ With a window of size 1, the channel is unchanged and $\mu_T(1)$ is equal to the total sinuosity of the original channel. Moving average on larger windows tend to straighten the channel by reducing the large deviations from the average channel orientation, until the point where very large windows result in a completely straight channel (total sinuosity of 1). The rate of decrease in the sinuosity (which we denote sinuosity plot) yields more information than only measuring the sinuosity as a single value.

At locations in the channel where there is a change in sign of the direction-change, one can define inflection points which are useful to define other parameters. The length of the channel between two successive inflection points is defined as the half-meander length λ_h, while the straight-line distance is Y_k (Figure 3). The straight-line distance between the inflection points that define a full meander is X_j (Figure 3). Based on these concepts, [*Howard and Hemberger*, 1991] introduce the full-meander sinuosity, μ_W, the half-meander sinuosity, μ_H, and the residual sinuosity, μ_R, defined as

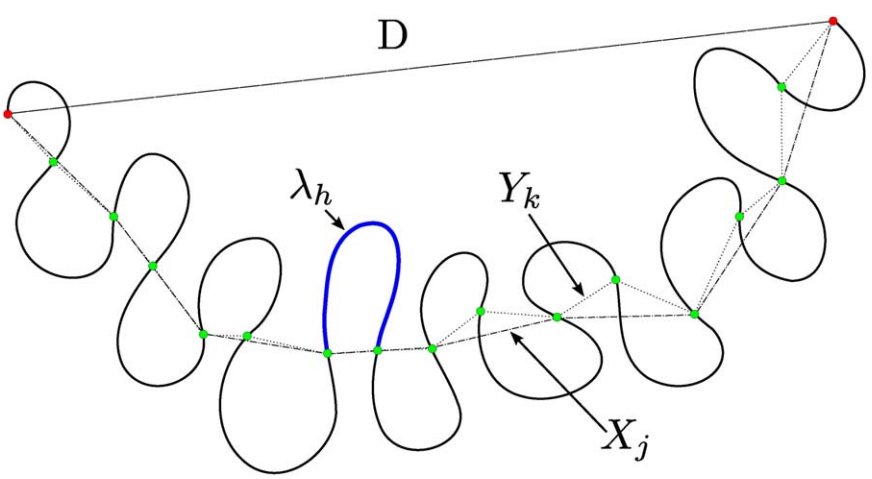

Figure 3. Parameters useful to define attributes of sinuosity and the half-meander quantities (modified from *Howard and Hemberger* [1991]).

$$\mu_w = \sum_{j=1}^{l} \frac{X_j}{D} \tag{1}$$

$$\mu_H = \frac{\sum_{k=1}^{m} Y_k}{\sum_{j=1}^{l} X_j} \tag{2}$$

$$\mu_R = \frac{\lambda}{\sum_{k=1}^{m} Y_k} \tag{3}$$

Often, the logarithm of these attributes offers a better representation. In the following, the superscript * is added to the notation when a logarithmic transformation is used.

Ferguson [1976] and *Howard and Hemberger* [1991] suggest the spectral analysis of the direction-change as another useful tool to characterize meandering channels. Here we compute the peak wavelength of the meandering λ_P and the average wavelength of meandering $\lambda_{\{av\}}$ as described in *Howard and Hemberger* [1991]. In addition to the spectral analysis, a number of standard statistical measures can be computed on the direction-change $\Delta\theta$, like the average value $\Delta\theta_{av}$, the standard deviation $\Delta\theta_{sd}$, the skewness $\Delta\theta_{sk}$, and the kurtosis $\Delta\theta_{kr}$.

Once half-meanders have been identified, a coefficient of asymmetry can be defined within the two inflection points at the location where the direction-change is maximum [see *Howard and Hemberger*, 1991, for details]. The point where the direction-change is maximum splits the half meander into two segments of length λ_u and λ_d, respectively, which can be used to define the asymmetry coefficient as $\mathcal{A}_h = (\lambda_u - \lambda_d)/\lambda_h$. Here we compute the mean and the median value of the asymmetry coefficient and the mean value of the half-meander length λ_h.

These attributes will be used to evaluate our proposed meandering channels simulation method and compare its results with seven real-world channels. The same 12 attributes are used to validate the results in all seven cases. While only a summary of the results is displayed in the body of this paper, an extensive summary of the outcomes is available as supporting information.

2.3. Unconditional Meandering Channel Simulation With Sequential Gaussian Simulation

Once the training channel is discretized as a series of directions, classical geostatistical simulation methods can be applied in 1-D to obtain alternative realizations of directions that correspond to realizations of meandering channels. A classical geostatistical approach would call for modeling the spatial structure of these directions with a variogram [*Gumiaux et al*., 2003], then using simulations methods such as Sequential Gaussian Simulation (SGS) [*Goovaerts*, 1997] to generate new models having similar properties. This is the approach adopted by *Oliver* [2002]. Since we are working in 1-D, simulation methods that are traditionally used in time series analysis such as the autoregressive family of models, could also be used to generate realizations of directions and, hence, realizations of channels. However, such approaches result in channels that do not present realistic meanders bends [*Georgsen and Omre*, 1993; *Oliver*, 2002]. This is caused by the use of Gaussian-based simulation methods that account mostly for lower-order statistics (i.e., pdf and variogram), and are hence unable to represent the complex successions of directions needed to obtain similar features than the ones occurring in natural systems. This is illustrated by one realization of a channel based on the directions statistics observed at Birch Creek, Alaska (Figure 4a). The use of SGS entails that low-order properties such as the histogram (Figures 4c and 4d) and the variogram of directions (Figure 4e) are reproduced. However, it is enough to look at the resulting channel (Figure 4b) to realize that the result is not satisfying, with a jaggy channel and a general aspect that does not conform to what is observed in Birch creek. Moreover, SGS requires that the data are Gaussian, which is not strictly the case here (Figure 4c). Histogram anamorphosis often needs to be applied, but it can lead to intractable artifacts when the data are back-transformed [*Kolbjørnsen and Abrahamsen*, 2004]. The detailed comparison of the individual attributes is available in the supporting information.

Another quantitative evaluation of the results obtained on this example is provided by plotting the total sinuosity computed on a moving window $\mu_T(w)$,which is poorly reproduced by the SGS-based simulation (Figure 4f). This example demonstrates that honoring low-order statistics at short distances does not guarantee adequate reproduction of the succession of directions in meandering channels.

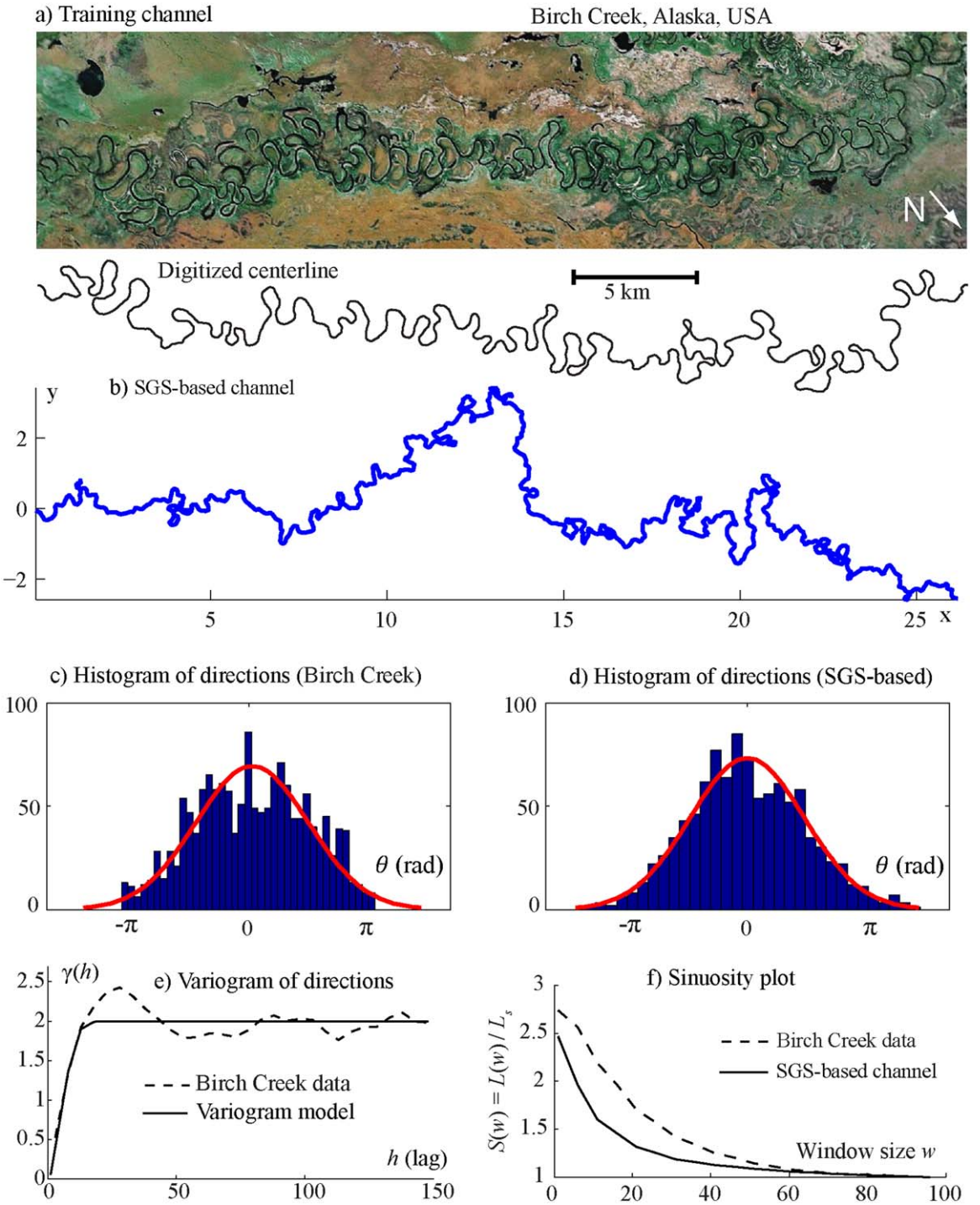

Figure 4. Channels simulated with unconditional SGS. (a) Birch Creek river training channel (Source: "Birch Creek, Alaska" 66°02′10N and 144°33′46W. Google Earth, 16 October 2013). (b) SGS-based simulation. (c and d) Histograms of original and SGS-simulated channels. (e) variograms (*h* is in unit of discretization steps). (f) Sinuosity plots (window size is in unit of discretization steps). *x* and *y* units are in km.

2.4. Unconditional Meandering Channel Simulation With DS

The idea pursued in this paper is that by using multiple-point statistics instead of variograms, one should be able to better reproduce the characteristics of meandering channels observed in the nature. The first implementations of MPS were limited to the simulation of categorical variables [e.g., *Strebelle*, 2002], making it difficult to represent directions, which are a continuous variable in the interval [0, 2π]. However, more

recent algorithms do accommodate continuous variables. In this study, we use the direct sampling (DS) to simulate successions of directions that present similar high-order patterns as the training image (in this case training channel). We refer the reader to [*Mariethoz et al*., 2010b] and subsequent applications [e.g., *Jha et al*., 2013; *Meerschman et al*., 2013] for a complete description of the algorithm, a pseudocode and parameterization guidelines. We only give a brief summary below.

The principle of DS is to sequentially simulate the values of an array of directions, given the statistical information provided by the directions of the training channel. It should be noted that since the approach is nonparametric, no normalization or variable transformation is necessary. Consider first the array of the training directions $\boldsymbol{\theta}^{TI}=\{\theta_1^{TI},\theta_2^{TI},\ldots,\theta_{N-1}^{TI}\}$ and the one to be simulated $\boldsymbol{\theta}^{SIM}=\{\theta_1^{SIM},\theta_2^{SIM},\ldots,\theta_{M-1}^{SIM}\}$. The numbers M and N of segments of the same length s that compose the simulated channel and the training channel can be different, as we can simulate a channel with the same statistical properties as the training one but with a different curvilinear length. The values of θ^{SIM} are obtained by sequentially drawing samples of the training channel θ^{TI} such that they are compatible with the previously drawn samples. Let $\theta\tilde{i}^{SIM}$ be an unknown value of direction, and suppose some direction values of θ^{TI} are known. We define $O_{\tilde{i},K}^{SIM}$ as the set containing the indexes of the K locations nearest to $\tilde{i}$ where a value of direction is known. The basic idea is to find, in the training channel, a location $\tilde{j}$ where the directions at the locations defined by the translated neighborhood $O_{\tilde{j},K}^{TI}$ are close enough to the ones at the locations $O_{\tilde{i},K}^{SIM}$. To define the concept of "close enough" we adopt two possible distance functions $d(.)$, and a threshold value t that defines when a distance is low enough for two patterns to be considered similar. The training channel is sampled at random locations until a location $\tilde{j}$ that satisfies $d(O_{\tilde{i},K}^{SIM},O_{\tilde{j},K}^{TI})<t$ is found. In that case, the value of $\theta\tilde{j}^{TI}$ is assigned to $\theta\tilde{i}^{SIM}$, and the simulation proceeds sequentially from another unknown value of direction. If no such location is found, the location with the smallest distance is used.

The important point is that using the first sample with a distance lower than t is equivalent to sampling from the underlying high-dimensional conditional distribution. The distance function $d(.)$ can be defined as any valid distance function between the arrays of direction values with indexes $O_{\tilde{i},K}^{SIM}$ and $O_{\tilde{j},K}^{TI}$. Some examples of distance are Euclidean, Manhattan, mean-invariant or transform-invariant. Considering alternative distances allows a high degree of flexibility, as demonstrated by the use of transform-invariant distances for geological modeling [*Mariethoz and Kelly*, 2011]. Here we adopt two possible distance definitions:

1. An Euclidean distance, for which two pieces of channels are close when they have similar geometry and similar direction. It has the following form

$$d\left(O_{\tilde{i},K}^{SIM},O_{\tilde{j},K}^{TI}\right)=\sqrt{\frac{1}{n}\sum_{i\in O_{\tilde{i},K}^{SIM},j\in O_{\tilde{j},K}^{TI}}^{K}\left[\theta_i-\theta_j\right]^2} \tag{4}$$

2. A mean-invariant Euclidean distance [*Mariethoz et al*., 2010b], which is a modified version of equation (4) where the terms to compare are centered on zero. The result is that only deviations from the mean are considered, and therefore patterns having different average value of $\overline{\theta}_{\tilde{i},K}^{SIM}$ and $\overline{\theta}_{\tilde{j},K}^{TI}$ can still be similar (here $\overline{\theta}_{\tilde{i},K}^{SIM}$ and $\overline{\theta}_{\tilde{j},K}^{TI}$ are the mean values of the directions with indexes contained in the sets $O_{\tilde{i},K}^{SIM}$ and $O_{\tilde{j},K}^{TI}$, respectively). In this case, two successions of directions are close when they correspond to two pieces of channels having similar geometry, but possibly different overall direction. This mean-invariant distance has the form

$$d\left(O_{\tilde{i},K}^{SIM},O_{\tilde{j},K}^{TI}\right)=\sqrt{\frac{1}{n}\sum_{i\in O_{\tilde{i},K}^{SIM},j\in O_{\tilde{j},K}^{TI}}^{K}\left[\left(\theta_i-O_{\tilde{i},K}^{SIM}\right)-\left(\theta_i-O_{\tilde{j},K}^{TI}\right)\right]^2} \tag{5}$$

Figure 5 illustrates the workflow for the simulation of one channel with either distance (4) or (5). Figure 5a shows the digitized Preacher Creek river, used as training channel. The channel is converted to an array of directions (Figure 5b), which constitutes the training channel.

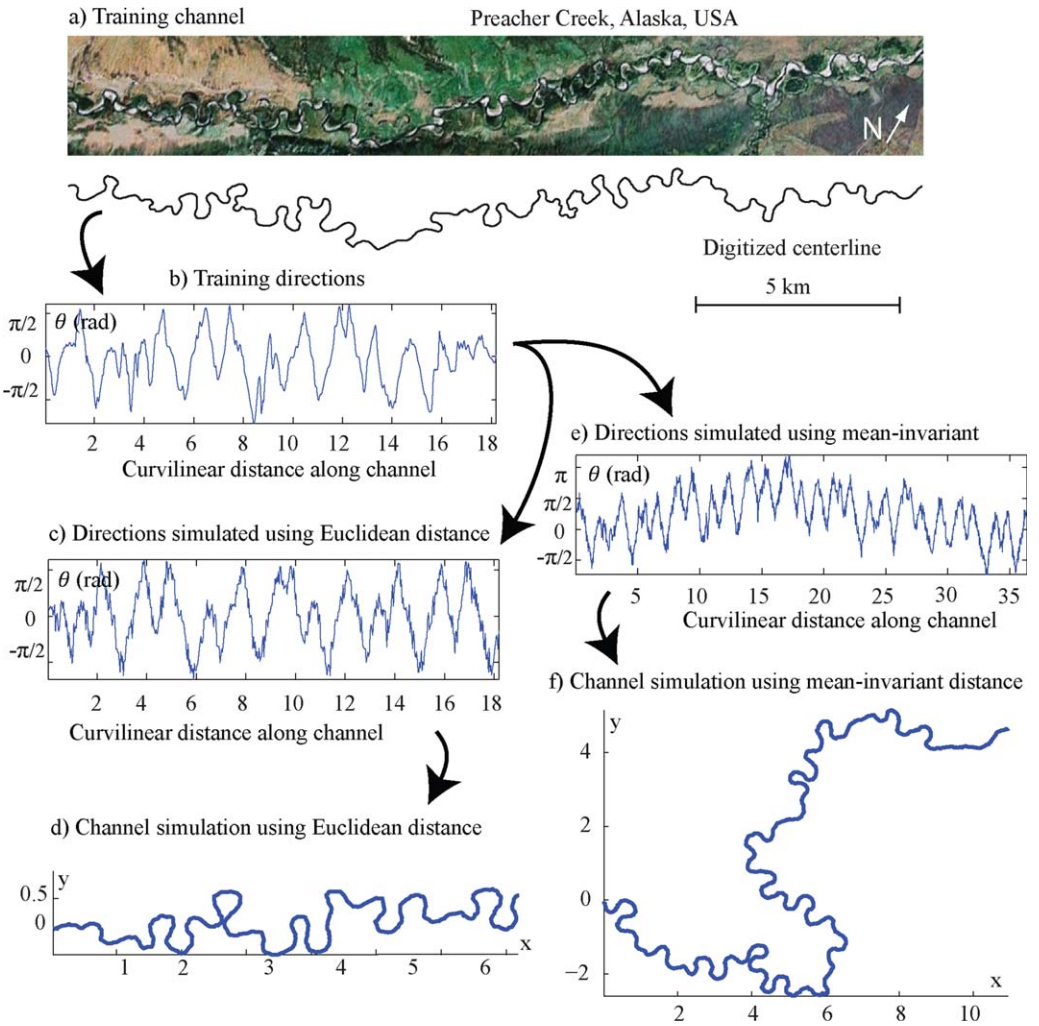

Figure 5. Workflow for unconditional channel simulation illustrated. (a) Preacher Creek river training channel (Source: "Preacher Creek, Alaska" 65°47′84N and 145°32′13W. Google Earth, 16 October 2013). (b) Training directions derived from training channel. (c and d) Channel simulation using Euclidean distance. (e and f) Channel simulation using mean-invariant Euclidean distance. *x* and *y* units are in km.

In a first case, this training channel is used to generate one realization of directions with the DS algorithm (Figure 5c) with the Euclidean distance (equation (4)). The simulated channel is presented in Figure 5d. At this stage, it should be noted that given the origin of the channel, the succession of directions in Figure 5c entirely characterizes the channel of Figure 5d. Since the simulated directions are distributed around zero, the general direction of the simulated channel is horizontal.

In a second case, a channel is generated with the same methodology, except that the mean-invariant Euclidean distance is used (equation (5)). The mean of the resulting simulated directions (Figure 5e) is not constrained any more around zero. Although the patterns are locally similar to the ones derived from the training channel (Figure 5b), their average can vary, resulting in an additional degree of freedom in the global direction of the simulated channel (Figure 5f).

There are thus two possible approaches to the simulation of unconditional meandering channels. The first one, using a Euclidean distance, allows obtaining stochastic channels having the same global direction as the training channel. The second approach, using a mean-invariant Euclidean distance, generates channels with no specified direction. In the following sections, we will show how the overall channel direction can be guided using conditioning data.

Table 1. Summary of the Morphometric Attributes Considered in the PCA

μ_T^*	Logarithm of the total sinuosity
μ_W^*	Logarithm of the full-meander sinuosity
μ_H^*	Logarithm of the half-meander sinuosity
μ_R^*	Logarithm of the residual sinuosity
λ_P	Peak wavelength of the meandering
$\lambda_{\{av\}}$	Average meandering wavelength
$\lvert\Delta\theta\rvert_{\{av\}}$	Absolute value of the direction-change, average
$\lvert\Delta\theta\rvert_{\{sd\}}$	Absolute value of the direction-change, standard deviation
$\lvert\Delta\theta\rvert_{\{sk\}}$	Absolute value of the direction-change, skewness
$\lvert\Delta\theta\rvert_{\{kr\}}$	Absolute value of the direction-change, kurtosis
$\lambda_{h\{av\}}$	Average half-meander length
$\mathcal{A}_{h\{av\}}$	Average asymmetry coefficient

It is also noted that the computational cost of the method is minimal since a simulation of a hundred channels takes few seconds on a standard CPU (2.3 GHz Intel Core i7), and can therefore be included in Monte-Carlo simulation frameworks for uncertainty quantification.

In order to compare the results of our method with the SGS-based approach of *Oliver* [2002] we performed a principal component analysis (PCA) for the Birch Creek case shown in Figure 4 [*Pedregosa et al*., 2011]. This PCA, performed using 12 of the aforementioned morphometric attributes summarized in Table 1, is a general way of evaluating synthetic channels and to compare them with natural ones [*Howard and Hemberger*, 1991]. The results (Figure 6) confirm the poor performance of the SGS over the DS, with in particular the SGS-based channels clustered together far from the reference, whereas DS provides a larger ensemble of models that encompasses the reference. The increased spread of the ensemble is of particular interest to correctly represent the geological uncertainty in application of alluvial reservoir modeling.

A more detailed analysis of the results of the PCA shows that the first component accounts for the 93% of the variance, and for this component the variable with the largest influence is the average half-meander length (see supporting information Table S1, for the detailed results of the PCA). For two of the cases considered (Bubye River and Mamore River), the most important variable is the half-meander length, while for the remaining five test cases the peak wavelength of meandering dominates.

2.5. Conditional Meandering Channel Simulation

It is useful in practice that realistic-looking meandering channels trajectory can be controlled to pass through locations where the occurrence of a channel is known. For example, there may be boreholes where

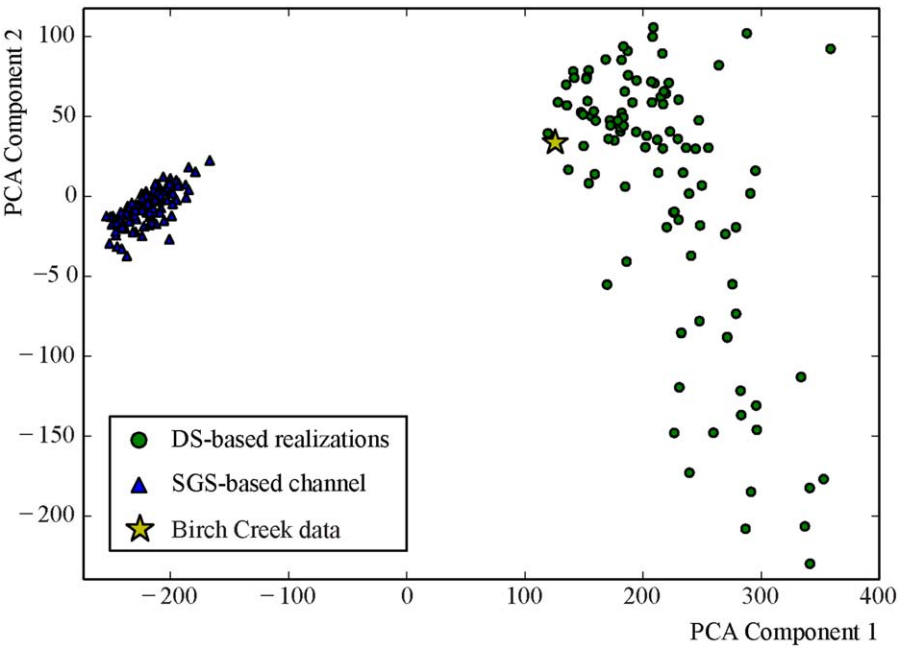

Figure 6. Principal component analysis comparing 100 unconditional simulation with SGS, 100 unconditional simulations with DS and the reference values of the training channel (Birch Creek, Alaska). Note that the axes do not represent physical units because in a PCA the data are normalized then represented in a transformed space.

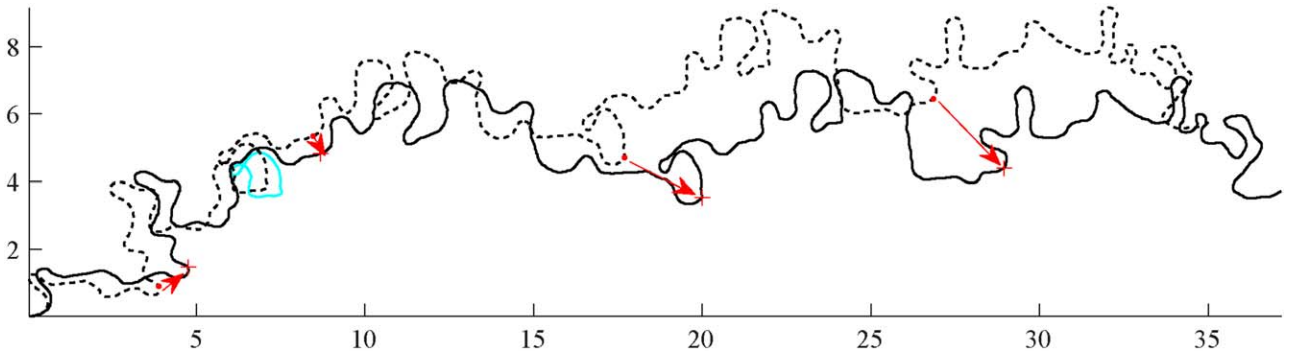

Figure 7. Trend-based conditioning. Dotted line: unconditional channel simulated based on the Birch Creek training channel. Solid line: conditional channel. Red crosses: conditioning data. Blue line: meander shut close because of the conditioning process. Arrow shows the channel displacement caused by the trend. *x* and *y* units are in km.

sand and gravel intervals have been identified, and it is desirable to condition the simulated channels to pass there.

However, the nature of the method makes any local conditioning a challenge. The position of each point depends on the integral of all preceding directions along the channel. Therefore, the final channel can be largely affected by a single direction value that can for example bend the subsequent parts of the channel away from conditioning data.

2.5.1. Trend-Based Conditioning

One possible conditioning method was proposed by *Oliver* [2002] in the context of Gaussian-based channels. It consists in adding a trend on an unconditional channel, such that the trend cancels the errors to the conditioning points, as illustrated in Figure 7. The points of the unconditional channel closest to the observed ones are selected, and the trend is applied to adjust the channel to pass through the observed locations. However, in cases where the channel displays complex structures, nothing ensures the physical consistency of such an additive trend. Therefore, the results may present artifacts, such as meanders that are stretched open or collapsed shut, creating self-intersections in the channel (shown in blue in Figure 7). Another drawback is that the morphological properties (i.e., the aforementioned measures of sinuosity) of the channel can be modified. Moreover, in cases where the conditioning data are relatively far from the unconditional channel, the resulting important trend values can incur extreme distortions in the channel.

The trend method can be appropriate in cases where the conditioning data are already very close to the unconditional channel, i.e., where a slight trend is sufficient. In the general case, however, the trend method is not viable and an alternative conditioning strategy constrained by realistic patterns is sought.

2.5.2. Conditioning by ISR

The principle of the conditioning methodology adopted here is to iteratively perturb a channel until it honors the conditioning locations. However, the perturbations have to be incurred in such a way that the channel remains realistic. In our context, a simulation is considered realistic when it respects the statistics of the direction patterns found in the training image. These statistics are represented by the aforementioned morphometric attributes.

One method that has been successful to accomplish such perturbations is the iterative spatial resampling scheme (ISR), which has been applied in the context of hydrogeological inverse problems [*Mariethoz et al*., 2010a]. Its principle is to start with an unconditional realization, then randomly select a number of points in it that are imposed as conditioning data for a new simulation—using identical training image or spatial model. The resulting model can be again resampled. The resampling and simulation steps are iterated, yielding a chain of models that all have similar characteristics as the training channel, but vary locally from one iteration to the next. It has been shown by *Mariethoz et al*. [2010a] that the patterns obtained at each ISR iteration are coherent, in a Bayesian sense, with the prior information given by the training image/training channel.

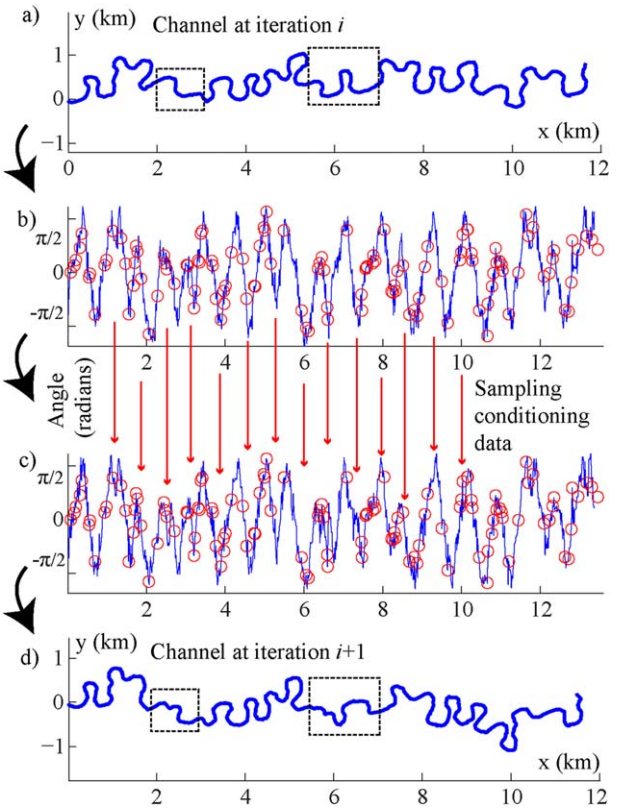

Figure 8. Illustration of the ISR applied to meandering channels. (a) Initial channel simulated based on the Preacher Creek training channel. (b) Corresponding directions, resampled to obtain a new realization (c). (d) Perturbed channel.

Figure 8 illustrates ISR perturbation applied to the simulation of a meandering channel. The algorithm starts with an initial channel (Figure 8a), which is converted to directions as discussed in section 2.1.. A fraction φ of these directions is then randomly chosen (Figure 8b). These samples are used as conditioning data in the DS algorithm for a new simulation of directions (Figure 8c). The samples are represented as red circles and are identical in Figure 8b and in Figure 8c. These correspond to locations that are "frozen" between iteration i and iteration $i + 1$. The remainder of the new realization is resimulated and hence can change from one iteration to the next. The channel corresponding to iteration $i + 1$ (Figure 8d) is similar to the channel if iteration i with respect to the types of structures and the location of these structures, but can present local differences, as highlighted by dotted boxes on Figure 8d.

Using this method, channels can be conditioned to local data by using an acceptation/rejection criterion that preferentially accepts channels improving the match to the data. This results in a chain of channel models with progressively increasing match to the data, which ends when the error is under a given error tolerance e_t.

However, if resampling occurs on the entire channel length, as in Figure 8, directions may be modified at the beginning of the channel, resulting in the entire remaining part of the channel to be rotated. This modifies the location of certain locations that have been conditioned in previous iterations of ISR, causing the optimization to never reach convergence. Hence, the strategy adopted here is to process a limited channel section at a time, each time conditioning to a single conditioning location.

For each channel section, a chain of models is generated, each corresponding to one iteration i and having an associated error to the data $e(i)$. This error is calculated as the smallest distance between the simulated channel section and the conditioning point considered:

$$e(i) = \min_{\text{section}} \sqrt{(x_i - x_d)^2 + (y_i - y_d)^2} \quad (6)$$

x_d and y_d being the coordinates of the conditioning point and x_i and y_i being the coordinates of the point of the channel section simulated at iteration i and closest to (x_d, y_d). Each new model is accepted only if it is the best matching in the chain, i.e., if the error $e(i)$ is lower than the error of all previous models 1, . . ., $i - 1$. This ensures that the chain of channel sections gets closer and closer to the data point, until an error under e_t is reached, which is the stopping criterion. Note that here we use a strategy that seeks to systematically minimize the error, but a Metropolis-based approach could have been used instead [*Mosegaard and Tarantola*, 1995].

The corresponding channel section is then accepted and the algorithm moves on to the next section. In order to accelerate the convergence of the conditioning, the resampled fraction φ is progressively increased, such as to incur large perturbations in case of a large misfit, and smaller perturbations when fine-tuning the segment to closely improve the match to a given data point. The resampled fraction φ changes at each iteration and is calculated as

$$\varphi(i) = \min\left(\frac{e_t}{e(i)}, \varphi_{\max}\right). \quad (7)$$

φ_{max}, corresponds to the maximum resampling fraction to be used, defined here as 0.1 which corresponds to resampling 10% of all values in a channel section. Such a resampling fraction (illustrated in Figure 8) ensures that significant changes in the channel are always possible. It was found that larges values, such as 0.5 or 0.75, result in very little change from one iteration to the next, and therefore very slow convergence. In the initial iterations, $e(i)$ is much larger than e_t, resulting in the first term in equation (7) to be small, therefore yielding low $\varphi(i)$ and ensuring that large changes are possible in the channel section. As the data match improves, φ progressively increases up to the value φ_{max}.

The curvilinear channel length between one conditioning point and the next is initially unknown because it will depend on the number of meanders bends present in the section after conditioning. Hence, during the conditioning process, the total channel length is progressively incremented by an amount larger than the linear distance to the next conditioning point times the channel total sinuosity observed in the training channel. This ensures that the algorithm does not overshoot by producing an unnecessarily large section to reach a nearby data point. In certain cases, it is possible that the ISR does not converge and fails to condition to a location. This happens in cases where the direction of the previous section makes it very difficult for the channel to reach the next data point, for example because the location of the conditioning points are aligned in a way that is not compatible with the training channel. In such cases, the previous section is unsimulated after a maximum allowed number of iterations and the process starts again from the beginning of this previous section. In our tests, we found that a maximum number of 50 iterations generally gives good results.

The MPS simulation of channel directions is one-dimensional and therefore computationally very light. In general, a single iteration takes a fraction of a second. Hence, although this inverse-based conditioning method is iterative, it is still faster than traditional applications of MPS (such as in the example of Figure 1).

Figure 9 shows the result of a conditional channel using the Preacher Creek River as training channel. Two scenarios of conditioning locations are considered, corresponding to two different usages of the conditional simulation approach. In the first case (Figure 9a), the data represent hypothetical measurements, and are disposed such that the channel cannot at the same time strictly honor these locations ($e_t = 0.1$ km) and conserve the overall straight direction observed in the training channel. This is, however, achieved by using the mean-invariant Euclidean distance (equation (5)), which is able to produce a channel that honors all data and reproduces the training channel features.

In the second case (Figure 9b), the data do not correspond to measurements, but to anchoring locations that are designed to provide guidance on the general channel direction. Here again a mean-invariant Euclidean distance is used, but the conditioning is not strict ($e_t = 2$ km), rather designed to delineate, for example, the general direction of a paleovalley.

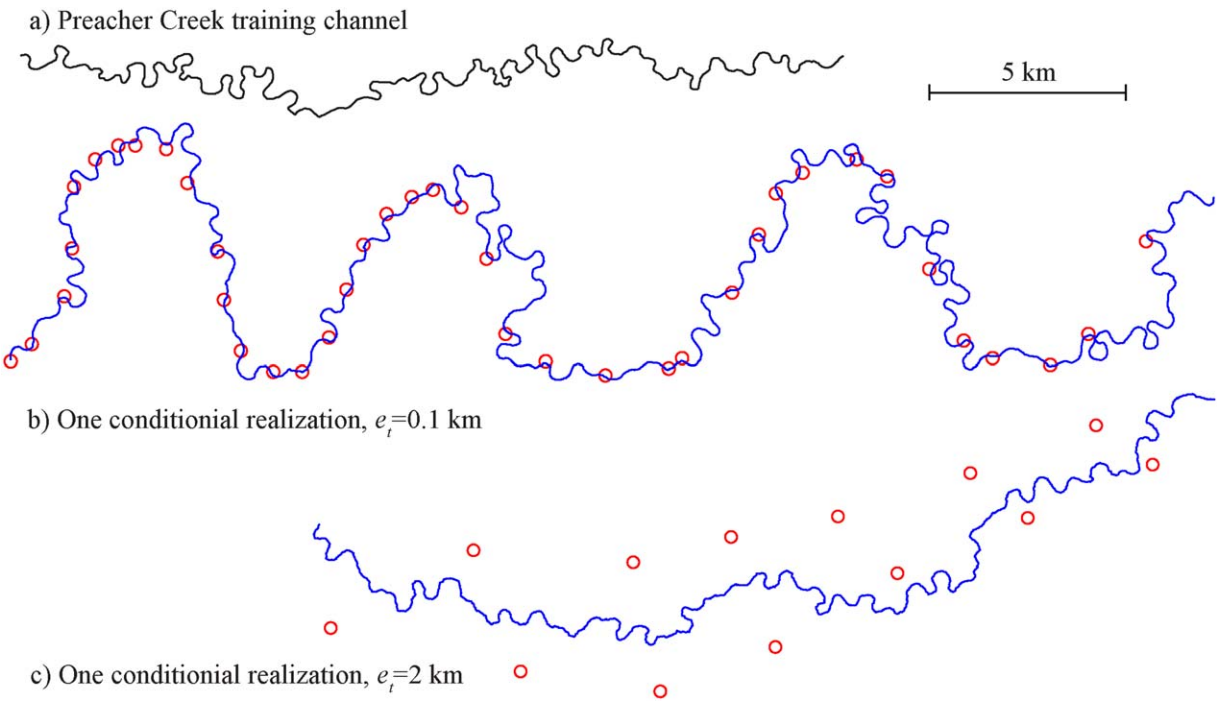

Figure 9. (a) Digitized training channel (Preacher Creek case study). (b and c) Two conditional simulations performed with different values of the error tolerance $\boldsymbol{e_t}$.

Statistics about morphometric attributes are computed in the unconditional case and on realizations conditioned to 10 locations. It is found that the conditioning procedure does not significantly affect the patterns reproduction, which is fairly similar to what is observed in the training channel. Variograms, sinuosity plots, and PCA based on morphometric attributes are displayed in Figure 10 for 100 realizations based on the Birch Creek case, along with a comparison with the Gaussian case of Figure 4.

Additional examples of the conditional simulation procedure can be found in the supporting information videos S1 and S2. Variograms, sinuosity plots, box plots of six important morphometric attributes and PCA allow verifying that, overall, the statistical properties of the training channel are respected and that the conditioning process does not introduce any significant bias in the simulations. Note that the variables that have an important weight in determining the first three components of the PCA are the same if the PCA is performed on the 100 unconditional or on the 100 conditional simulations (see supporting information table and figures).

For a more detailed and systematic analysis, six morphometric attributes, considered by *Howard and Hemberger* [1991] as important to discern natural occurring meandering channels from simulated ones, have been computed for 100 unconditional and conditional DS simulations, for all seven case studies. The detailed results are presented in the supporting information Figures S3–S22. It results that the statistics of the direction patterns are not significantly affected by the conditioning procedure, and that our method is generally able to reproduce well the characteristics of the training channel.

In the case of the total sinuosity, the conditional simulation performs better than the unconditional one. This is due to the choice of the conditioning points along the same direction as the training channel, while for the unconditional simulation the channel can evolve freely an potentially result in a total sinuosity that differs from the one of the training channel. Nevertheless, from the point of view of all the other sinuosity measures (full, half-meander, and residual), the results of conditional and unconditional simulations are comparable (only the half-meander sinuosity is shown here). In terms of peak wavelength, both conditional and unconditional simulations have median values that are within 5 m or less from the reference values.

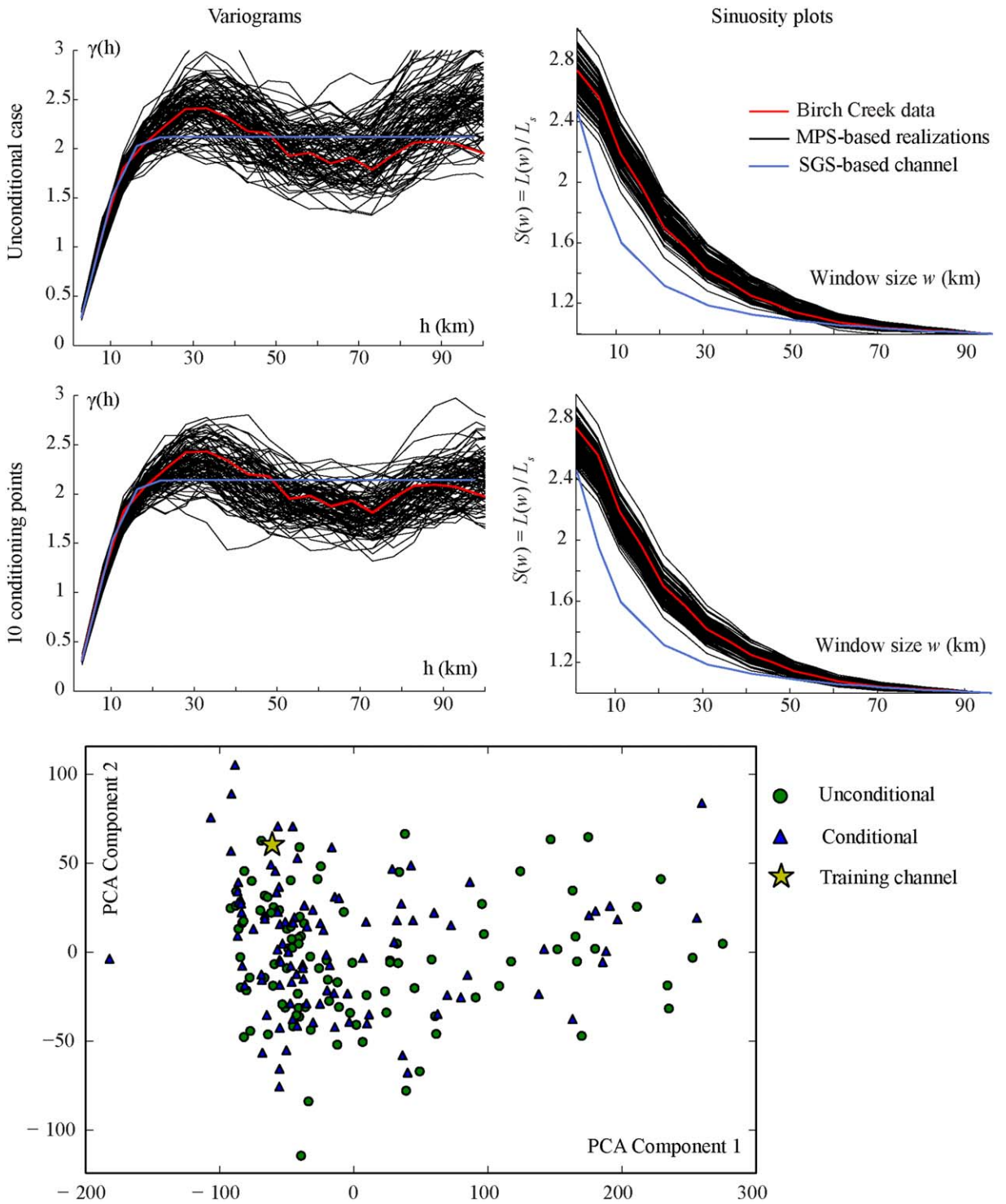

Figure 10. The effect of conditioning on patterns reproduction. Comparison of 100 unconditional realizations with 100 realizations conditioned to 10 points, for the Birch Creek data. The four subplots in the top of the figure compare the variograms and sinuosity plots. The bottom subplot shows a PCA performed on the same 100 conditional and unconditional realizations of the Birch Creek river, using the morphometric attributes introduced in the text.

This discrepancy increases in the case of the average wavelength: conditional and unconditional simulations are always comparable, but the deviation of the median values from the reference is then over 10 m. A satisfactory result is obtained for the average half-meander length, where both conditional and unconditional simulations have a median value within a 10% error margin around the reference value. Another

interesting result is obtained for the average value of the asymmetry index: overall, other simulation techniques rarely reproduce the sign of this variable observed on natural channels [*Howard and Hemberger*, 1991], while with the DS simulations capture the correct sign of this variable in six out of seven case studies.

An important result is that in the PCA performed using the aforementioned morphometric attributes, conditional and unconditional simulations are well mixed and the reference training channel is correctly included in the ensemble of simulations. This is true for all seven case studies, indicating that our method performs well across the range of indicators considered.

It should be noted here that the approach adopted, i.e., consisting in conditioning one data point at a time, implies that the points are in a given order. For cases where the conditioning points represent measurements (Figure 9a), wells data often inform the presence or absence of a channel at a given location, but do not provide information regarding the order of the data along a channel. It is our opinion that in the absence of other information, the order of the data along the channel is mostly an interpretative decision. For example in Figure 9, one may decide that there is a single channel with an overall sinusoid shape, or several relatively straight channels parallel to each other. The data alone do not allow deciding between these possibilities, and several scenarios could be investigated, which should be essentially driven by a geologist's decision. Additionally, one may not know whether different channels measurement belong to the same channel or not. In the instances where geochronological data are available, it may be possible to group channel points by similarity in age. In most practical cases however, the point data have to be randomly attributed to individual channels at each realization.

3. Conclusion

This work presents a new perspective on the application of multiple-point statistics, made possible by the flexibility provided by the Direct Sampling method. It is applied outside the standard context of spatially localized patterns and categorical variables. Instead, the principle is to simulate meandering channel centerlines by a 1-D succession of continuous direction that are nonlocalized.

The stochastic simulation framework presented for meandering channels simulation overcomes some of the difficulties inborn in commonly used models. Contrarily to physically based or cellular automata models, there is no need to define parameters and rules for the model, since the statistical properties are inferred directly from the properties of real-world channels, from which all the statistical features are extracted. The added value of our approach is that it allows integrating expert knowledge in the modeling process though the choice of a training channel, which it otherwise very difficult to express quantitatively. Additional input can be given by conditioning data to guide the overall channel geometry. Moreover, our approach allows quantifying geological uncertainty through the use of Monte-Carlo simulations.

The simulated channels present a high degree or realism and include nonlinear features typical of real-world channels. The model is not based on physical equations representing the evolution of a meandering channel, but instead mimics the spatial characteristics observed on present-day rivers, which is a rich and widely available source of information.

The methodology has been illustrated using examples coming from digitized rivers taken in different environments. It performed well in all cases considered, with simulations of stochastic channels that preserve the observed features as well as statistical characteristics, and allow conditioning to locations with known channel occurrence. Conditioning is accomplished with an inverse procedure based on the Iterative Spatial Resampling method. It was shown that such conditioning is also possible in cases where the direction of the channel differs from the direction of the training channel, through the use of mean-invariant Euclidean distances. Conditioning can be used either to constrain channels to measured data, or to guide the overall direction of the simulated channels, where the data are then used as anchoring locations rather than hard data. The resulting simulations could be used, for example, to generate geological structures for input to hydrogeological models, to design synthetic hydrologic networks for catchment studies or as elementary pieces to build 3-D training images for classical MPS applications. For example, the method of *Comunian et al*. [2012] allows obtaining 3-D models from orthogonal 2-D cross sections. It is however difficult to apply because while it is relatively straightforward to obtain vertical sections perpendicular to the channels, it is more difficult to obtain horizontal sections. Our method can fill this gap.

Another example is object-based methods, where a current challenge is to create objects that are conditioned to dense data sets. Our method is ideal to create channelized objects that are conditional by construction. Using the classical Boolean framework [*Lantuejoul*, 2002], it is possible to stochastically stack these channels in order to obtain 3-D models of alluvial reservoirs.

Alternatively, our model could be used as starting point for physically based models such as the one of *Ikeda et al*. [1981] or as a first channel skeleton required for cellular models [*Coulthard and Van De Wiel*, 2006; *Coulthard et al*., 2007], for genetic models [*Gross and Small*, 1998] or object-based models [*Comunian et al*., 2011].

The limited computational requirements of the methodology allows to easily integrate it in inverse simulation procedures, and future research will focus on the application of these techniques to account for different types of data such as, for example, geophysical measurements that indicate the general direction and location of channel belts.

One limitation of the model is that the channel centerline does not evolve during time, such as, for example, when one considers the evolution of a meandering channel on geological time scales [*Seminara*, 2006; *Van De Wiel et al*., 2011]. However, by providing training channels at different stages of their evolution (or corresponding to different climatological conditions) one can potentially simulate different depositional stages. Similarly, questions of nonstationarity may complicate the application of the approach. In this regard the solutions classically implemented in MPS to deal with nonstationarity can be used [*Hu and Chugunova*, 2008]. When the training channel is nonstationary and one wants stationary simulations, the approach of *Chugunova and Hu* [2008] using an auxiliary variable would be appropriate. When nonstationary simulations are sought based on several stationary training channels, the simulated domain could be partitioned in subdomains that each use a different training channel [*de Vries et al*., 2009]. For example, if a delta is to be modeled accounting for the progradation of the sediments, a training channel to use for the deep parts of the reservoir would correspond to the downstream part of a river system, whereas for the shallow part of the reservoir one should use training channels coming from the upper parts of a catchment. Another limitation related to the conditioning approach is that the order of the data along the channel have to be known, and should be inferred by geological interpretation. This limitation, however, does not apply when the conditioning data are used as anchoring locations.

Future work will look at using our method to build 3-D volumes of deltaic reservoirs in a real setting and compare the results with the architectures obtained from process-based models. Our method could then prove a faster method for modeling such reservoirs, which would moreover allow for conditioning. Another avenue is the use of the generate channels as flexible object in 3-D Boolean simulation methods.

Acknowledgments
This work was supported by the Australian Research Council, the National Water Commission, and the Groundwater Education Investment Fund and by a scholarship of the Chilean government. The authors also thank Bryce F. Kelly for valuable discussions.

References

Bashore, W., U. Araktingi, M. Levy, and U. Schweller (1994), *Importance of a geological framework for reservoir modelling and subsequent fluid-flow predictions, in AAPG Computer Application in Geology*, edited by J. M. Yarus and R. L. Chambers, pp. 159–175, Am. Assoc. of Pet. Geol., Tulsa, Okla.

Bertoncello, A., T. Sun, H. Li, G. Mariethoz, and J. Caers (2013), Conditioning surface-based geological models to well and thickness data, *Math. Geosci.*, *45*(7), 873–893.

Camporeale, C., P. Perona, A. Porporato, and L. Ridolfi (2005), On the long-term behavior of meandering rivers, *Water Resour. Res.*, *41*, W12403, doi:10.1029/2005WR004109.

Castilla-Rho, J. C., G. Mariethoz, B. F. J. Kelly, and M. S. Andersen (2014), Stochastic reconstruction of paleovalley bedrock morphology from sparse datasets, *Environ. Modell. Software*, *53*, 35–52.

Chugunova, T., and L. Hu (2008), Multiple-point simulations constrained by continuous auxiliary data, *Math. Geosci.*, *40*(2), 133–146.

Comunian, A., P. Renard, J. Straubhaar, and P. Bayer (2011), Three-dimensional high resolution fluvio-glacial aquifer analog. Part 2: Geostatistical modeling, *J. Hydrol.*, *405*(1–2), 10–23.

Comunian, A., P. Renard, and J. Straubhaar (2012), 3D multiple-point statistics simulation using 2D training images, *Comput. Geosci.*, *40*, 49–65.

Coulthard, T. J., and M. J. Van De Wiel (2006), A cellular model of river meandering, *Earth Surf. Processes Landforms*, *31*(1), 123–132.

Coulthard, T. J., D. M. Hicks, and M. J. Van De Wiel (2007), Cellular modelling of river catchments and reaches: Advantages, limitations and prospects, *Geomorphology*, *90*(3–4), 192–207.

Crosato, A. (2008), *Analysis and Modelling of River Meandering*, IOS Press, Amsterdam.

Darby, S. E., A. M. Alabyan, and M. J. Van de Wiel (2002), Numerical simulation of bank erosion and channel migration in meandering rivers, *Water Resour. Res.*, *38*(9), 1163, doi:10.1029/2001WR000602.

de Vries, L., J. Carrera, O. Falivene, O. Gratacos, and L. Slooten (2009), Application of multiple point geostatistics to non-stationary images, *Math. Geosci.*, *41*(1), 29–42.

Deutsch, C. V., and L. Wang (1996), Hierarchical object-based geostatistical modeling of fluvial reservoirs, *Math. Geol.*, *28*(7), 857–880.

Deutsch, C. V., and T. T. Tran (2002), FLUVSIM: A program for object-based stochastic modeling of fluvial depositional systems, *Comput. Geosci.*, *28*(4), 525–535.

Einstein, A. (1926), The cause of the formation of meanders in the courses of rivers and of the so-called Baer's Law, *Die Naturwiss.*, *14*, 653–684.

Ferguson, R. (1976), Disturbed periodic model for river meanders, *Earth Surf. Processes Landforms*, *1*(4), 337–347.
Frisch, U., B. Hasslacher, and Y. Pomeau (1986), Lattice-gas automata for the Navier-Stokes equation, *Phys. Rev. Lett.*, *56*(14), 1505–1508.
Georgsen, F., and H. Omre (1993), Combining fiber processes and Gaussian random functions for modeling fluvial reservoirs, in *Proceedings: Geostatistics Tróia '92*, edited by A. Soares, pp. 425–440, Kluwer Academic, Dordrecht, Netherlands.
Goovaerts, P. (1997), *Geostatistics for Natural Resources Evaluation*, 496 pp., Oxford Univ. Press, Oxford, U. K.
Gross, L. J., and M. J. Small (1998), River and floodplain process simulation for subsurface characterization, *Water Resour. Res.*, *34*(9), 2365–2376.
Gumiaux, C., D. Gapais, and J. Brun (2003), Geostatistics applied to best-fit interpolation of orientation data, *Tectonophysics*, *376*(2003), 241–259.
Gyr, A. (2010), The meander paradox-a topological view, *Appl. Mech. Rev.*, *63*(2), 1–12.
Haldorsen, H. H., and D. M. Chang (1986), Notes on stochastic shales from outcrop to simulation models, in *Reservoir Characterization*, edited by L. W. Lake and H. B. Carrol, pp. 152–167, Academic, New York.
Howard, A. D., and A. T. Hemberger (1991), Multivariate characterization of meandering, *Geomorphology*, *4*(3–4), 161–186.
Howard, A. D., and T. R. Knutson (1984), Sufficient conditions for river meandering: A simulation approach, *Water Resour. Res.*, *20*(11), 1659–1667.
Hu, L., and T. Chugunova (2008), Multiple-point geostatistics for modeling subsurface heterogeneity: A comprehensive review, *Water Resour. Res.*, *44*, W11413, doi:10.1029/2008WR006993.
Ikeda, S., G. Parker, and K. Sawai (1981), Bend theory of river meanders. 1: Linear development, *J. Fluid Mech.*, *112*, 363–377.
Jha, S., G. Mariethoz, J. P. Evans, and M. McCabe (2013), Demonstration of a geostatistical approach to physically-consistent downscaling of climate modeling simulations, *Water Resour. Res.*, *49*, 1–14, doi:10.1029/2012WR012602.
Keogh, K. J., A. W. Martinius, and R. Osland (2007), The development of fluvial stochastic modelling in the Norwegian oil industry: A historical review, subsurface implementation and future directions, *Sediment. Geol.*, *202*(1–2), 249–268.
Klise, K., G. Weissmann, S. McKenna, E. Nichols, J. Frechette, T. Wawrzyniec, and V. Tidell (2009), Exploring solute transport and streamline connectivity using lidar-based outcrop images and geostatistical representations of heterogeneity, *Water Resour. Res.*, *45*, W05413, doi:10.1029/2008WR007500.
Kolbjørnsen, O., and P. Abrahamsen (2004), Theory of the cloud transform for applications, in *Geostatistics Banff 2004*, edited by O. Leuangthong and C. V. Deutsch, pp. 45–54, Kluwer Acad., Berlin.
Koltermann, C., and S. Gorelick (1996), Heterogeneity in sedimentary deposits: A review of structure-imitating, process-imitating, and descriptive approaches, *Water Resour. Res.*, *32*(9), 2617–2658.
Lancaster, S. T., and R. L. Bras (2002), A simple model of river meandering and its comparison to natural channels, *Hydrol. Processes*, *16*(1), 1–26.
Langbein, W. B., and L. B. Leopold (1966), River meanders—Theory of minimum variance, *U.S. Geol. Surv. Prof. Pap., 422-H*, 1–15.
Lantuejoul, C. (2002), *Geostatistical Simulation: Models and Algorithms*, 232 pp., Springer, Berlin.
Le Coz, M., P. Genthon, and P. M. Adler (2011), Multiple-point statistics for modeling facies heterogeneities in a porous medium: The Komadugu-Yobe Alluvium, Lake Chad Basin, *Math. Geosci.*, *43*(7), 861–878.
Lopez, S. (2003), Modélisation de réservoirs chenalisés méandriformes, Approche génétique et stochastique, doctoral thesis, 276 pp., Sch. of Mines., Paris.
Lopez, S., I. Cojan, J. Rivoirard, and A. Galli (2008), Process-based stochastic modelling: Meandering channelized reservoirs, *Spec. Publ. Int. Assoc. Sedimentol.*, *144*, 139–144.
Mariethoz, G., and B. F. J. Kelly (2011), Modeling complex geological structures with elementary training images and transform-invariant distances, *Water Resour. Res.*, *47*, W07527, doi:10.1029/2011WR010412.
Mariethoz, G., P. Renard, and J. Caers (2010a), Bayesian inverse problem and optimization with Iterative Spatial Resampling, *Water Resour. Res.*, *46*, W11530, doi:10.1029/2010WR009274.
Mariethoz, G., P. Renard, and J. Straubhaar (2010b), The direct sampling method to perform multiple-point geostatistical simulations, *Water Resour. Res.*, *46*, W11536, doi:10.1029/2008WR007621.
Meerschman, E., G. Pirot, G. Mariethoz, J. Straubhaar, M. Van Meirvenne, and P. Renard (2013), A practical guide to performing multiple-point statistical simulations with the Direct Sampling algorithm, *Comput. Geosci.*, *52*, 307–324.
Michael, H., A. Boucher, T. Sun, J. Caers, and S. Gorelick (2010), Combining geologic-process models and geostatistics for conditional simulation of 3-D subsurface heterogeneity, *Water Resour. Res.*, *46*, W05527, doi:10.1029/2009WR008414.
Mosegaard, K., and A. Tarantola (1995), Monte Carlo sampling of solutions to inverse problems, *J. Geophys. Res.*, *100*(B7), 12,431–12,447.
Murray, A. B., and C. Paola (1994), A cellular model of braided rivers, *Nature*, *371*(6492), 54–57.
Murray, A. B., and C. Paola (1997), Properties of a cellular braided-stream model, *Earth Surf. Processes Landforms*, *22*(11), 1001–1025.
Oliver, D. (2002), Conditioning channel meanders to well observations, *Math. Geol.*, *34*, 185–201.
Parker, G., Y. Shimizu, G. V. Wilkerson, E. C. Eke, J. D. Abad, J. W. Lauer, C. Paola, W. E. Dietrich, and V. R. Voller (2011), A new framework for modeling the migration of meandering rivers, *Earth Surf. Processes Landforms*, *36*(1), 70–86, doi:10.1002/esp.2113.
Pedregosa, F., et al. (2011), Scikit-learn: Machine learning in Python, *J. Mach. Learn. Res.*, *12*, 2825–2830.
Perucca, E., C. Camporeale, and L. Ridolfi (2005), Nonlinear analysis of the geometry of meandering rivers, *Geophys. Res. Lett.*, *32*, L03402, doi:10.1029/2004GL021966.
Posner, A. J., and J. G. Duan (2012), Simulating river meandering processes using stochastic bank erosion coefficient, *Geomorphology*, *163–164*, 26–36.
Pyrcz, M., J. Boisvert, and C. Deutsch (2009), ALLUVSIM: A program for event-based stochastic modeling of fluvial depositional systems, *Comput. Geosci.*, *35*(8), 1671–1685, doi:10.1016/j.cageo.2008.09.012.
Renard, P., and D. Allard (2013), Connectivity metrics for subsurface flow and transport, *Adv. Water Resour.*, *51*, 168–196.
Renard, P., J. Straubhaar, J. Caers, and G. Mariethoz (2011), Conditioning facies simulations with connectivity data, *Math. Geosci.*, *43*(8), 879–903.
Schlüter, S., and H. J. Vogel (2011), On the reconstruction of structural and functional properties in random heterogeneous media, *Adv. Water Resour.*, *34*(2), 314–325.
Seminara, G. (2006), Meanders, *J. Fluid Mech.*, *554*, 271–297.
Seminara, G., and M. B. Pittaluga (2012), Reductionist versus holistic approaches to the study of river meandering: An ideal dialogue, *Geomorphology*, *163–164*, 110–117.
Seminara, G., G. Zolezzi, M. Tubino, and D. Zardi (2001), Downstream and upstream influence in river meandering. Part 2: Planimetric development, *J. Fluid Mech.*, *438*, 213–230.

Stien, M., P. Abrahmsen, R. Hauge, and O. Kolbjørnsen (2007), Modification of the snesim algorithm, paper presented at Petroleum Geostatistics 2007, EAGE, Cascais, Portugal, 10–14 Sep.

Stølum, H. H. (1996), River meandering as a self-organization process, *Science*, *271*(5256), 1710–1713.

Strebelle, S. (2002), Conditional simulation of complex geological structures using multiple-point statistics, *Math. Geol.*, *34*(1), 1–22.

Strebelle, S., and N. Remy (2005), Post-processing of multiple-point geostatistical models to improve reproduction of training patterns, in *Geostatistics Banff 2004*, edited by O. Leuangthong and C. V. Deutsch, pp. 979–988, Springer, Dordrecht, Netherlands.

Sun, T., P. Meakin, T. Jøssang, and K. Schwarz (1996), A simulation model for meandering rivers, *Water Resour. Res.*, *32*(9), 2937–2954.

Surkan, A. J., and J. Van Kan (1969), Constrained random walk meander generation, *Water Resour. Res.*, *5*(7), 1343–1352.

Suzuki, S., and S. Strebelle (2007), Real-time post-processing method to enhance multiple-point statistics simulation, paper presented at Petroleum Geostatistics 2007, EAGE, Cascais, Portugal, 10–14 Sep.

Van De Wiel, M. J., T. J. Coulthard, M. G. Macklin, and J. Lewin (2011), Modelling the response of river systems to environmental change: Progress, problems and prospects for palaeo-environmental reconstructions, *Earth Sci. Rev.*, *104*(1–3), 167–185.

Zinn, B., and C. Harvey (2003), When good statistical models of aquifer heterogeneity go bad: A comparison of flow, dispersion, and mass transfer in connected and multivariate Gaussian hydraulic conductivity fields, *Water Resour. Res.*, *39*(3), 1051, doi:10.1029/2001WR001146.